Scanning Tunneling Microscopy of Insulators and Biological Specimens Based on Lateral Conductivity of Ultrathin Water Films

Reinhard Guckenberger,* Manfred Heim, Gregor Cevc, Helmut F. Knapp, Winfried Wiegräbe, Anton Hillebrand

Scanning tunneling microscopy is based on the flow of an electrical current and thus cannot be used to directly image insulating material. It has been found, however, that a very thin film of water (about one monolayer) adsorbed to a surface exhibits a surprisingly high conductivity that is sufficient to allow scanning tunneling microscope imaging at currents below 1 picoampere. Hydrophilic insulators, such as glass and mica, can thus be imaged in humid air. The same is true for biological specimens deposited on such surfaces, as demonstrated by the scanning tunneling microscope imaging of plasmid DNA on mica.

Scanning tunneling microscopy (STM) has become an indispensible tool of surface science that can provide atomic resolution on flat surfaces. The only prerequisite is sufficient electrical conductivity of the sample. Thus, insulators cannot be imaged by conventional STM and it is difficult to apply this technique to the study of biological materials because of their notoriously poor conductivity. Only organic samples thinner than about 1 nm, which allow tunneling through the material, can routinely be imaged with good results. Thicker specimens need to be coated with at least 1 nm of metal. However, the thickness and the granular structure of such films prevent high resolution in the resulting STM images. Efforts have been made, therefore, to image biological material without coating [see (*1*) and (*2*) for reviews]. The results, to date, have often been disappointing, and many researchers in biology have turned their efforts toward atomic force microscopy (AFM).

Interestingly, a dependence of STM imaging on humidity was found in several STM experiments (*3*–*7*). These observations as well as general considerations (8, 9) have led us to speculate that an adsorbed water film might be responsible for the observed conductivity [*1*, *3*, *7*; see also (*10*)].

Our present experimental studies show that the presence of one monolayer of water at the investigated surface is sufficient for successful STM imaging of insulating material such as glass and mica at low current. Similarly, various biological samples can be imaged by STM in humid air, even when supported by an insulator. We demonstrate this with STM images of uncoated plasmid DNA on mica. These results open up a wide field of new applications for STM in materials science and in biology. Many materials can now be studied by means of STM that previously could only be imaged with AFM. This development offers new opportunities because STM involves a different contrast mechanism and uses other imaging conditions in terms of applied forces and tips than AFM. Besides application for STM imaging, the unexpected high conductivity of ultrathin water films is also of fundamental interest.

The STM instrument used for our experiments is described in (*11*). Important features are (i) provisions to control the humidity of the ambient air and (ii) the use of a very sensitive preamplifier, which allows us to take images at tunneling currents as low as 0.05 pA (*12*) (for integration times of seconds, one can measure currents even down to 2 fA). The tips used in our experiments are prepared by electrochemical etching of tungsten wire (*13*). The samples are fixed mechanically onto a sample holder made of stainless steel, which also provides electrical contact to the sample side facing the tip.

We performed two types of experiments with this instrument: (i) measurement of the surface conductivity of bulk insulators as a function of the humidity of the ambient air, and (ii) STM imaging of such surfaces and of several biological samples prepared on mica. For conductivity measurements on mica, glass, and lipid films, STM feedback was switched off and the tip was brought into mechanical contact with the sample. In this way, any tunneling resistance was avoided. The contact area of the tip, however, could have varied considerably. Therefore, Pt-C electrodes of well-defined geometry were prepared by vacuum coating in additional experiments. A circular mask with a diameter of 3 mm and with a hole in its center 0.3 mm in diameter was used to leave a ring-shaped area of uncoated mica. Electrical connection to the central electrode was achieved by mechanical contact with the tunneling tip. For all preparations, we first cleaned mica in air to create a freshly exposed surface. Glass cover slips were rendered hydrophilic by glow discharge (1 min) in a plasma cleaner.

Figure 1 represents a typical conductivity measurement on the mica sample with Pt-C electrodes. It shows the dependence of the steady-state current on ambient humidity. For similar samples the curves are reproducible to within 30%. However, the current values decrease by one order of magnitude within 1 day, further decrease being much slower. When freshly cleaved mica samples without any coating were brought into direct contact with the tunneling tip, curves similar to those in Fig. 1 were obtained but with currents smaller by factors of up to 10. Furthermore, the currents vary considerably from tip to tip, but not between different positions on the mica for a given tip. Glass surfaces that were exposed to glow discharge showed higher conductivities than mica. On glass, typical currents at 1 V were 0.5 pA at 40% relative humidity (RH) and 20 pA at 60% RH.

Similar conductivity measurements were also made with mica-supported Langmuir-Blodgett (LB) films of dipalmitoylphosphatidylcholine (DPPC) and dipalmitoylphosphatidylethanolamine (DPPE). No current could be detected in monolayers that are known to present their hydrophobic tails toward the air. For preparations in which a layer of DPPC or DPPE was transferred as a second layer on top of a DPPE monolayer, a humidity-dependent current could be measured. The observed current was similar to that given in Fig. 1 in the case of a DPPC layer on top of a DPPE layer but was much smaller for a symmetric DPPE bilayer. The observed conductivity of these bilayers can be attributed to the polar head groups that point into the air. A detailed

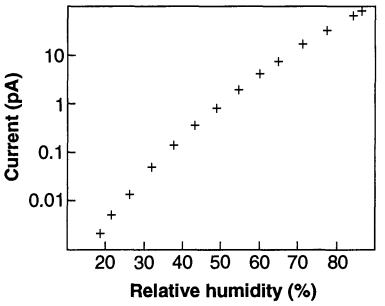

Fig. 1. Effect of ambient humidity on the surface conductivity of mica between Pt-C electrodes. After each increment of humidity, we allowed an equilibration time of 20 min before recording the current. The applied bias was 1 V.

R. Guckenberger, H. F. Knapp, W. Wiegräbe, A. Hillebrand, Max-Planck-Institut für Biochemie, D-82152 Martinsried, Germany.
M. Heim and G. Cevc, Medizinische Biophysik, Klinikum rechts der Isar, Technische Universität München, D-81675 München, Germany.

*To whom correspondence should be addressed.

account of these experiments on lipids is given elsewhere (*14*).

Most of the measured currents were well within the range of tunneling currents over which our STM instrument can be operated in the imaging mode. Consequently, it was possible to image glass, mica, and lipid bilayers on mica by STM, provided that the set point of the tunneling current was chosen to be smaller than the currents measured with the tip in mechanical contact.

This result encouraged us to also use mica as a substrate for biological specimens. Plasmid DNA [pUC18 (*15*)] was prepared on mica as follows: A small drop (2 μl) of the DNA solution [10 mM tris-HCl, 1 mM EDTA, lyophilized and resuspended in pure water (18.2 megohm·cm)] was placed on a piece of freshly cleaved mica and left to adsorb for about 1 min. We then washed the sample by placing it on top of a large drop of pure water for 5 s and then blotting off the water with a filter paper. The same procedure was also used to prepare type IV collagen and tobacco mosaic virus (TMV) on mica.

Figures 2 and 3 show the corresponding STM images of the plasmid DNA on mica. The step on the right side in Fig. 2 represents just one mica layer, 1 nm in height. Two plasmid loops spread across this step. Inside these loops, the substrate appears lower than outside the plasmid loops, indicating differences in conductivity. Figure 3 illustrates the lateral resolution obtained so far. The part of the DNA shown in the inset has an apparent width of 3.5 nm, which is close to its true diameter of about 2.5 nm. The scans can be repeated several times for stable tips, without noticeable changes in the images. Both polarities of the sample voltage can be used; in general, imaging is more stable at negative sample bias than at positive. Collagen and TMV are also easily imaged by the same STM technique (*16*).

The lateral conductivity of all investigated surfaces strongly depends on ambient humidity. This conductivity is obviously correlated with the adsorption of water to the surface. The average thickness of the water layer on a mica surface depends on the RH of the ambient air (*17*). It ranges from 0.15 nm at 45% RH to 0.4 nm at 70% RH. According to our current measurements, such a thin water layer exhibits a surprisingly high conductivity, larger than that of bulk water by up to five orders of magnitude. This result may be related to the known effect of structuring of water at surfaces. The conclusion that water plays the major part in the observed conductivity is supported by another aspect of the experiments with LB films of phospholipids: DPPC head groups are known to be hydrated much more than the less hydrophilic DPPE head groups (*18*). This finding correlates well with the lateral conductivities we have measured.

With respect to STM imaging, the water film on the surface of a hydrophilic insulator can be considered to function as a conductive coat, similar to the metal coat that is usually used for STM on insulating material. Because the water film can be much thinner, a higher lateral resolution can be expected. The details visible in Fig. 3 are very encouraging. The resolution is higher than in previous STM images of uncoated biological specimens taken under conditions similar to those used in Fig. 3 but prepared on Pt-C–coated mica (*3*, *4*, *7*, *19*). In these earlier experiments, the tip-substrate distance was at least 5 nm, thus preventing high resolution. For the same voltage, current, and humidity, the tip-substrate distance is presumably much smaller on plain mica, as indicated by a much smaller variation of the vertical tip position for changes of the tunneling voltage.

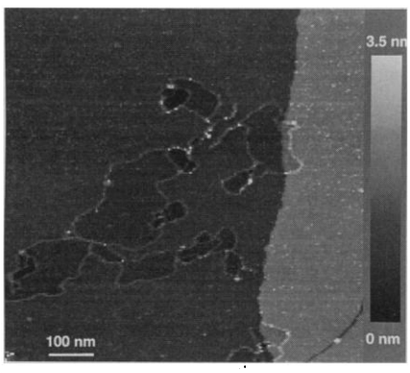

Fig. 2. Plasmid DNA (pUC18) adsorbed to mica, imaged by STM in humid air. The 1-nm step at the right side corresponds to the thickness of one mica layer. The dark line at the bottom right represents a crack in the mica. Imaging conditions: tunneling current, 0.25 pA; sample bias, −2.5 V; RH, 66%.

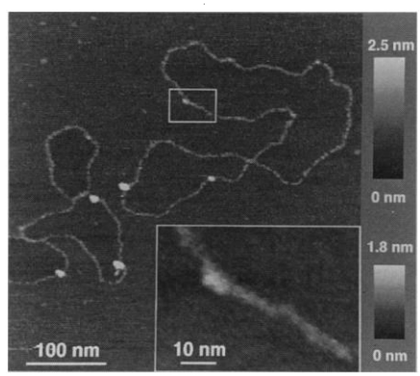

Fig. 3. Plasmid DNA (pUC18) on mica imaged by STM at high resolution. The box in the overview marks the area displayed in the inset. This inset is a cutout of a zoomed-in image taken immediately after the overview. Imaging conditions: tunneling current, 0.5 pA; sample bias, −7 V; RH, 65%.

The heights measured in the images of DNA were always smaller than the known molecular thicknesses. The largest average height we have measured with plasmid DNA to date is 1.2 nm; this is about one half of the true diameter. Presumably related to this problem are the differences in the measured height levels of the substrate inside and outside the plasmid loops (see Fig. 2), which can be observed at conditions close to the limit of conductivity. The tunneling voltage in Fig. 2 was 2.5 V as compared with 7 V in Fig. 3. The DNA seems to act as a lateral conductivity barrier. The reduced conductivity of DNA as compared to mica may be caused by different amounts of adsorbed water. The DNA, acting as a resistor, will cause a difference in the local voltage inside and outside a plasmid loop, which in turn would reduce the height levels measured inside (*7*, *19*). The transverse resistance of a loop consisting of DNA will be larger for a small circumference, in agreement with the larger depth visible in Fig. 2 for small loops. A reduced conductivity over the DNA would also diminish the height of the molecule itself in the images. In contrast to DNA, images of TMV on mica gave height values relatively close to the known particle diameter (15 nm instead of 18 nm).

One of the main questions left open is the mechanism of humidity-dependent conductivity itself. One possibility is that proton conductivity is involved (*20*), perhaps proton hopping along structured water at surfaces. Other ions present may also move along hydrophilic surfaces. Another question concerns the gap between tip and sample that may be bridged by water, as proposed earlier as a mechanism for imaging biological material (*10*). More experiments are necessary to answer these questions.

Our observation of a surprisingly high conductivity of ultrathin water films, naturally present on hydrophilic surfaces, opens up a wide field of new applications of STM. Biological material is especially suited for this technique of STM imaging because most biological surfaces are hydrophilic. Moreover, many biological specimens adsorb very well to mica, which now can be used as a substrate in STM. Mica has been widely used for specimen preparation in electron microscopy, and one can profit from the large experience gained in this field. Our STM images of plasmid DNA on mica clearly demonstrate the capability of the technique.

Our initial experiments with other biological macromolecules suggest that this STM mode is rather general. Practice will reveal the ultimate resolution limit, but we are confident that further improvement in resolution is achievable, because a water film of one monolayer already provides

enough conductivity for the STM experiments. Moreover, the dependence of the local surface conductivity on the individual hydrophilicity of the molecular groups located directly under the tip may provide new contrast mechanisms for the detection of individual segments in large molecules. Beyond these new possibilities for surface imaging and analysis, it may be possible to study the local properties of adsorbed water, especially those that are related to the mechanism of conductivity.

REFERENCES AND NOTES

1. R. Guckenberger, W. Wiegräbe, T. Hartmann, W. Baumeister, in *Scanning Tunneling Microscopy II*, R. Wiesendanger and H.-J. Güntherodt, Eds. (Springer, Berlin, 1992), pp. 52–98.
2. O. Marti and M. Amrein, Eds., *STM and SFM in Biology* (Academic Press, San Diego, 1993).
3. R. Guckenberger *et al.*, *Ultramicroscopy* **31**, 327 (1989).
4. Z. Wang, T. Hartmann, W. Baumeister, R. Guckenberger, *Proc. Natl. Acad. Sci. U.S.A.* **87**, 9343 (1990).
5. G. J. Leggett *et al.*, *J. Phys. Chem.* **97**, 8852 (1993).
6. L. Gathercole, M. J. Miles, T. J. McMaster, D. F. Holmes, *J. Chem. Soc. Faraday Trans.* **89**, 2589 (1993).
7. R. Guckenberger, F. Terán Arce, A. Hillebrand, T. Hartmann, *J. Vac. Sci. Technol. B* **12**, 1508 (1994).
8. G. Cevc, *Biochim. Biophys. Acta* **1031–3**, 311 (1990).
9. G. Cevc and A. A. Kornyshev, *J. Electroanal. Chem.* **330**, 407 (1992).
10. J.-Y. Yuan, Z. Shao, C. Gao, *Phys. Rev. Lett.* **67**, 863 (1991).
11. R. Guckenberger *et al.*, *Ultramicroscopy* **25**, 111 (1988).
12. Input stage (20-gigohm feedback resistor) commercially available from Quintenz Hybridtechnik, Kramerstrasse 3, D-82061 Neuried, Germany.
13. B. Hacker, A. Hillebrand, T. Hartmann, R. Guckenberger, *Ultramicroscopy* **42–44**, 1514 (1992).
14. M. Heim, G. Cevc, R. Guckenberger, H. F. Knapp, in preparation.
15. A. Schaper, L. I. Pietrasanta, T. M. Jovin, *Nucleic Acids Res.* **21**, 6004 (1993).
16. R. Guckenberger *et al.*, in preparation.
17. D. Beaglehole, E. Z. Radlinska, B. W. Ninham, H. K. Christenson, *Phys. Rev. Lett.* **66**, 2084 (1991).
18. G. Cevc, in *Hydration of Biological Macromolecules*, E. Westhof, Ed. (Macmillan, New York, 1993), pp. 338–390.
19. R. Guckenberger *et al.*, *J. Vac. Sci. Technol. B* **9**, 1227 (1991).
20. D. B. Kell, *Bioelectrochem. Bioenerget.* **27**, 235 (1992).

21. We thank A. Schaper for providing the pUC18 plasmid DNA and T. Hartmann and R. M. Glaeser for valuable discussions. This work was supported by the Deutsche Forschungsgemeinschaft (SFB-266).

5 July 1994; accepted 4 October 1994

Atomic Control of the $SrTiO_3$ Crystal Surface

Masashi Kawasaki, Kazuhiro Takahashi, Tatsuro Maeda, Ryuta Tsuchiya, Makoto Shinohara, Osamu Ishiyama, Takuzo Yonezawa, Mamoru Yoshimoto, Hideomi Koinuma

The atomically smooth $SrTiO_3$ (100) with steps one unit cell in height was obtained by treating the crystal surface with a pH-controlled NH_4F-HF solution. The homoepitaxy of $SrTiO_3$ film on the crystal surface proceeds in a perfect layer-by-layer mode as verified by reflection high-energy electron diffraction and atomic force microscopy. Ion scattering spectroscopy revealed that the TiO_2 atomic plane terminated the as-treated clean surface and that the terminating atomic layer could be tuned to the SrO atomic plane by homoepitaxial growth. This technology provides a well-defined substrate surface for atomically regulated epitaxial growth of such perovskite oxide films as $YBa_2Cu_3O_{7-\delta}$.

In spite of enormous efforts since the discovery (*1*) and thin-film preparation (*2*) of high-temperature (high-T_c) superconducting oxides, nobody has succeeded in the preparation of high-T_c Josephson tunnel junction, the key device for superconducting electronics. One of the primary reasons is the unavailability of a device-quality single-crystal substrate. In view of such short coherence length of high-T_c superconductors (roughly 0.3 to 2 nm), both of the superconducting (S) and insulating (I) layer surfaces in SIS tunnel junction must be regulated on an atomic scale. Overcoming this severe requirement will require a substrate with excellent lattice matching and an atomically regulated surface.

The commercially available single-crystal oxide wafers are prepared by so-called mechanochemical polishing with an alkaline solution containing colloidal silica particles. As an example, the atomic force microscopy (AFM) image of an $SrTiO_3$ wafer surface is depicted in Fig. 1A. The surface has a small corrugation of 0.2 to 0.8 nm and is as smooth as that of Si wafer without any special treatment. However, this surface was not sufficiently smooth for using atomic layer epitaxy to deposit various oxide materials. Extensive studies on high-T_c superconductors and related oxide thin films are now enabling atomic layer-by-layer growth of these films, as verified by the observation of intensity oscillations in reflection high-energy electron diffraction (RHEED) (*3*, *4*). This technology is expected to explore a novel field of ceramics research because of its ability to artificially construct new compounds and devices (*5*). The substrate most frequently used is $SrTiO_3$, and it must be clean and have an atomically smooth surface. The in situ cleaning procedures, such as heating in an oxygen flow (*6*), ion bombardment cleaning (*7*), and sublimation of a Bi film deposited on $SrTiO_3$ (*8*) were reported to be effective for the former purpose because carbon-containing impurities could be removed from the surface. However, these processes cannot improve the surface smoothness. Thus, the surface roughness shown in Fig. 1A must be overcome by a new method.

The crystal structure of $SrTiO_3$ is of the perovskite type and consists of alternating stacks of SrO and TiO_2 atomic layers. If one could find a wet solution that dissolves one of the atomic layers but not the other atomic layer, one should be able to prepare an atomically smooth surface terminated by the latter atomic layer. Because SrO is a basic oxide and TiO_2 is an acidic oxide, controlling the pH of the wet etch solution may accomplish this purpose.

Buffered NH_4F-HF (BHF) solutions with various pH values were tested in this study. The NH_4F concentration was kept at 10 M. The $SrTiO_3$ substrates with (100) polished planes were immersed in the BHF solutions for 10 min, rinsed with pure water and ethanol, and dried in a nitrogen stream. The AFM image taken in air for the substrate treated with a BHF (pH = 4.5) solution is shown in Fig. 1B. This image shows that the surface is composed of steps and atomically flat terraces. The step height was 0.4 nm, which corresponded to the unit cell length of $SrTiO_3$. Such images were reproducibly observed on the entire surface of the substrates treated with BHF solutions (pH = 4.4 to 4.6). The ratio of the step height to the terrace width (150 nm) gives an off angle of 0.15°, which is in good agreement with the value determined by the x-ray diffraction. For the wafers treated by the BHF solutions with pH > 5, island-like residues of 0.2 to 0.4 nm in height were observed on the terraces. By treating the wafer in solutions with pH < 4, surfaces similar to that shown in Fig. 1B were obtained, but square etch pits were present. We presume that crystal defects and polishing damage are responsible for the etch pits.

The atomic smoothness of the substrate surface treated with BHF (pH = 4.5) was

M. Kawasaki, PRESTO, JRDC, and Research Laboratory of Engineering Materials, Tokyo Institute of Technology, Nagatsuta, Midori, Yokohama, 226 Japan.
K. Takahashi and T. Yonezawa, Shinkosha Co., Ltd., Sakae-ku, Yokohama, 247 Japan.
T. Maeda, R. Tsuchiya, M. Yoshimoto, H. Koinuma, Research Laboratory of Engineering Materials, Tokyo Institute of Technology, Nagatsuta, Midori, Yokohama, 227 Japan.
M. Shinohara and O. Ishiyama, Keihanna Research Laboratory, Shimazu Corp., Sorakugun, Kyoto 619-02, Japan.